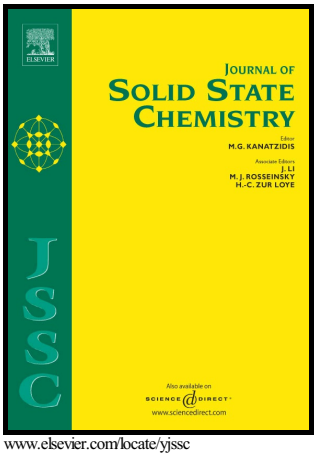


www.elsevier.com/locate/yjssc

# Chalcogenides as Thermoelectric Materials

Yixuan Shi, Cheryl Sturm, Holger Kleinke

PII: S0022-4596(18)30522-X
DOI: https://doi.org/10.1016/j.jssc.2018.10.049
Reference: YJSSC20488

To appear in: *Journal of Solid State Chemistry*

Received date: 10 September 2018
Revised date: 22 October 2018
Accepted date: 29 October 2018

Cite this article as: Yixuan Shi, Cheryl Sturm and Holger Kleinke, Chalcogenides as Thermoelectric Materials, *Journal of Solid State Chemistry,* https://doi.org/10.1016/j.jssc.2018.10.049

# Chalcogenides as Thermoelectric Materials

Yixuan Shi, Cheryl Sturm, Holger Kleinke*

Department of Chemistry and Waterloo Institute for Nanotechnology, University of Waterloo, Waterloo, ON, Canada N2L 3G1.

*To whom correspondence should be addressed. kleinke@uwaterloo.ca



**Abstract**

Thermoelectric materials can be utilized to generate electricity from a temperature gradient, thereby recycling the nowadays abundant waste heat, as well as for cooling applications by creating a temperature gradient from electricity. The former is based on the Seebeck effect, and the latter on the Peltier effect. Noticing the continuously declining fossil fuel resources and mankind's increasing need for energy, the importance for clean thermoelectric energy generation continues to climb.

Traditional thermoelectric materials were based on the binary tellurides $Bi_2Te_3$ and PbTe, which have been utilized for decades. The focus on tellurium as the heaviest non-radioactive chalcogen stems from the observation that heavier elements are advantageous for a reduced thermal conductivity, which is essential for the thermoelectric energy conversion. Moreover, tellurides are less ionic than sulfides or selenides, which leads to an enhanced carrier mobility that is advantageous for the desired high electrical conductivity. This review presents these traditional routes to low thermal conductivity, as well as alternatives based on the lighter analogues of tellurium, namely sulfur and selenium.

**Graphical Abstract:**

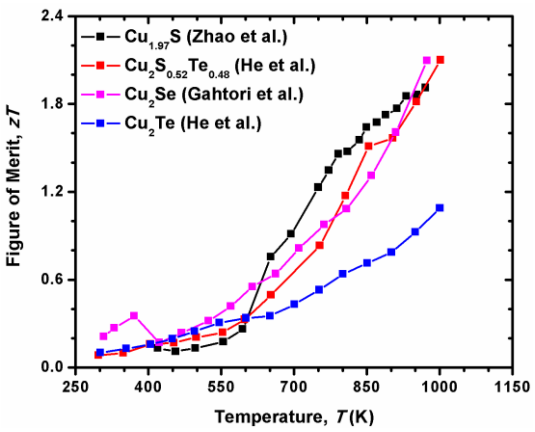


In special cases like in these binary copper chalcogenides, sulfides and selenides can outperform the more traditional thermoelectric tellurides.

*Keywords:* thermoelectric; energy; chalcogenide; crystal structure; physical properties.



## 1. Introduction

Because of the continuously declining natural resources and mankind's increasing need for electricity, more sustainable energy creation methods such as thermoelectric energy generation have become increasingly important [1]. Thermoelectric (TE) materials can create electricity via the Seebeck effect from a temperature gradient, which was first noticed by Seebeck in 1821, while the other direction – create a temperature gradient from electricity – is called Peltier effect [2,3]. Most notably, this method of energy generation has been in continuous use in space crafts since the early 1960s [4,5]. Since the better of two decades, TEs are at the

forefront of research into utilizing the waste heat in automotives to reduce the load on the alternator, and for waste heat utilization in stationary applications as well [5–8].

Thermoelectric devices consist of alternating *n*- and *p*-doped semiconducting legs, where the electrons in the *n*-type legs move like the holes in the *p*-type legs with the heat flow. The efficiency of the power generation $\eta$ is related to the device's average figure of merit *ZT*, written as $\overline{ZT}$ in equation (1) (with $T_H$ = hot temperature, $T_C$ = cold temperature), which in turn is the average of the materials' figure of merit, *zT* (equation (2)). Therein, *T* denotes the average temperature, $\alpha$ the Seebeck coefficient, $\sigma$ the electrical conductivity, and $\kappa$ the thermal conductivity. The power factor *P.F.* (equation (3)) is the product of $\alpha^2$ and $\sigma$, describing the electrical performance of a thermoelectric material.

$$\eta = \frac{T_H - T_C}{T_H} \frac{\sqrt{1+\overline{ZT}}-1}{\sqrt{1+\overline{ZT}}+\frac{T_C}{T_H}} \quad \text{Eq. (1)}$$

$$zT = T\alpha^2\sigma\kappa^{-1} \quad \text{Eq. (2)}$$

$$P.F. = \alpha^2\sigma \quad \text{Eq. (3)}$$

All these physical properties are functions of the charge carrier concentration, *n*. While the Seebeck coefficient generally decreases with *n*, both the electrical and the thermal conductivity increase with *n*. The increase of the electrical and the thermal conductivity with *n* can be illustrated via equations (4) - (6). Therein, *e* denotes the charge of an electron, $\mu$ the carrier mobility, $\kappa_L$ and $\kappa_e$ the lattice and the electronic thermal conductivity, respectively, and $L_0$ the Lorenz number. Equation (6) is known as the Wiedemann-Franz law. Equations (4) – (6) can be combined into equation (7) to summarize the dependence of the total thermal conductivity on the carrier concentration.

$$\sigma = n\, e\, \mu \quad \text{Eq. (4)}$$

$$\kappa = \kappa_L + \kappa_e \quad \text{Eq. (5)}$$

$$\kappa_e = L_0\, \sigma\, T \quad \text{Eq. (6)}$$

$$\kappa = \kappa_L + L_0\, n\, e\, \mu\, T \quad \text{Eq. (7)}$$

The different dependences of these key properties on the charge carrier concentration demonstrate why no one property can be optimized without negatively affecting at least another one. $\kappa_L$ constitutes an exception, as it can be minimized by working with heavy elements, such as thallium, lead, bismuth, antimony and tellurium without a detrimental impact on the other properties, and complex crystal structures, though they normally cause a low mobility of the charge carriers, detrimental to the electric conductivity [9,10].

Increasing $\overline{ZT}$ results in higher efficiency $\eta$ (equation (1)). Leading bulk materials exhibit peak $zT$ values between 1.1 and 1.8, such as $Ba_{0.08}La_{0.05}Yb_{0.04}Co_4Sb_{12}$ [11], $Ba_8Ni_{0.31}Zn_{0.52}Ga_{13.06}Ge_{32.2}$ [12], $Yb_{14}Mn_{0.4}Al_{0.6}Sb_{11}$ [13], $Ti_{0.5}(Zr_{0.5}Hf_{0.5})_{0.5}NiSn_{0.998}Sb_{0.002}$ [14], $\beta$-$Zn_4Sb_3$ [15], $Tl_9Bi_{0.98}Te_6$ [16], $Tl_{8.05}Sn_{1.95}Te_6$ and $Tl_{8.10}Pb_{1.90}Te_6$ [17], $Tl_2Ag_{12}Te_{7.4}$ [18], $Tl_{0.02}Pb_{0.98}Te$ [19] and $Bi_2Te_3$ [20]. All of the above comprise the above-mentioned heavy elements, and most of them complex crystal structures, with the notable exceptions of PbTe and $Bi_2Te_3$ variants and the Half Heusler phase, $Ti_{0.5}(Zr_{0.5}Hf_{0.5})_{0.5}NiSn_{0.998}Sb_{0.002}$.

Utilizing various methods of nanostructuring, further improvements have been achieved. Several examples exceed $zT_{max}$ values of 2, namely superlattices of $Bi_2Te_3/Sb_2Te_3$ [21], co-doped PbTe with nanodomains [22], Na-doped PbTe with SrTe nanoadditions [23], superlattices of $PbSe_{0.98}Te_{0.02}$/PbTe [24], nanostructured $Cu_2Se$ [25] and $Cu_2Se/CuInSe_2$ nanocomposites [26].

The majority of the state-of-the-art thermoelectrics are tellurides, which fit nicely into this review on thermoelectric chalcogenides. Most recently, more focus was placed on materials containing sulfur and selenium instead of tellurium (such as the above mentioned $Cu_2Se$), the lighter homologues of tellurium, because of their higher availability, lower cost and lower toxicity. As these materials are composed of lighter elements, other mechanisms to achieve the required low thermal conductivity are required. This article is reviewing recent success with sulfides and selenides in comparison to the more traditional thermoelectric tellurides.

## 2. Traditional thermoelectric tellurides: PbTe and $Bi_2Te_3$

PbTe, once properly modified as both *n*- and *p*-type, exhibits outstanding thermoelectric properties at elevated temperatures, suitable for electricity generation from waste heat. PbTe-based thermoelectric generators have been used in several NASA space missions, from Transit 4A to Viking 2, and in the Mars rover Curiosity [27]. PbTe crystallizes in the rock salt structure with a melting point of 1200 K, and is a semiconductor with a direct band gap of 0.32 eV [28].

Its highly symmetric crystal structure is the opposite of a complex crystal structure often postulated to be ideal for thermoelectrics [9]. In part, its relatively low lattice thermal conductivity of 2.2 W $m^{-1}K^{-1}$ stems from its very high average molar mass of 167.4 g $mol^{-1}$.

A re-investigation of the properties of the historic *n*-type PbTe revealed $zT$ values ≈ 1.4 between 700 K and 850 K [29]. Introducing nanodomains caused a significant performance increase as reflected in a $zT_{max}$ = 2.2 at 800 K for co-doped $AgPb_{18}SbTe_{20}$ [22] [30]. Kanatzidis coined this family LAST-*m*, for Lead Antimony Silver Telluride, with *m* the amount of Pb per formula unit (18 in $AgPb_{18}SbTe_{20}$). Ag-Sb-rich nanodomains in an Ag-Sb-poor matrix significantly lowered the lattice thermal conductivity to $\kappa_L$ ≈ 0.8 W $m^{-1}K^{-1}$ at room temperature, compared to 2.2 W $m^{-1}K^{-1}$ for PbTe.

Spinodal decomposition, which is a decomposition of a metastable phase into two phases on the nanoscale, resulted in an ultralow room temperature thermal conductivity of $\kappa_L$ = 0.38 W $m^{-1}K^{-1}$ for I-doped $(Pb_{0.95}Sn_{0.05}Te)_{0.92}(PbS)_{0.08}$, contributing to $zT_{max}$ = 1.5 at 642 K [31]. The combination of nanostructuring via addition of nano-SrTe with mesostructuring via spark-plasma-sintering, SPS, culminated in an outstanding $zT_{max}$ = 2.2 at 900 K, along with $\kappa_L$ = 0.53 W $m^{-1}K^{-1}$ [23].

Recent investigations have shown that SnSe, a lighter homologue of PbTe crystallizing in a strongly distorted NaCl variant in two different modifications, can exhibit great thermoelectric properties as well. Despite its lower averaged molar mass of 98.8 g $mol^{-1}$ compared to 167.4 g $mol^{-1}$ in case of PbTe, its low thermal conductivity stems from a combination of strongly anharmonic and anisotropic bonding caused by the lone pair of $Sn^{2+}$, as reflected in its heavily distorted $SnSe_7$ polyhedron [32]. Measured on a single crystal along its *b* axis, a sensationally high $zT_{max}$ = 2.6 was determined at 973 K [33]. Polycrystalline samples exhibit lower performance, for a example with a peak $zT$ = 0.92 at 873 K [34], and 1.36 at 823 K after solvothermal synthesis [35].

$Bi_2Te_3$ is still the state-of-the-art TE material for cooling applications. Like PbTe, its structure consists of closest packed layers of the cations and anions, but with a more complex order of …Te-Bi-Te-Bi-Te… along the *c* axis. As a consequence, its transport properties are anisotropic as in the case of SnSe, meaning the thermoelectric performance depends on the direction of the heat and electron flow. $Bi_2Te_3$ is also like PbTe a narrow-gap semiconductor,

with 0.16 eV, and a melting point of 858 K [36]. Co-doping with the transition metal atoms Cu, Ag and Cd yielded $zT_{max}$ = 1.4 at 425 K [37].

As in the case of PbTe, nanostructuring caused further improvements for $Bi_2Te_3$ as well. Introducing nanostructures via recrystallization through hot-forging lowered the lattice thermal conductivity below $\kappa_L$ = 0.5 W $m^{-1}K^{-1}$, from $\kappa_L$ = 1.5 W $m^{-1}K^{-1}$ for bulk $Bi_2Te_3$, which gave $zT_{max}$ values at room temperature [38]. The $Bi_2Te_3/Sb_2Te_3$ superlattices with $zT_{max}$ = 2.4 [21] remain at the forefront of these materials since 2001, while $Bi_2Te_3$ nanowires as published in 2013 were also reported to exceed $zT$ = 2 at room temperature [39].

## 3. Thermoelectric thallium tellurides

Thallium tellurides have increasingly attracted attention since the report of (an extrapolated) $zT_{max}$ = 1.2 for zone-melted $Tl_9BiTe_6$ in the year 2001, with an ultralow lattice thermal conductivity of $\kappa_L$ = 0.4 W $m^{-1}K^{-1}$ [40]. In contrast to PbTe and $Bi_2Te_3$, this material is bestowed with a complex crystal structure as a consequence of distorted coordination polyhedra around the thallium atoms, whereas Pb is surrounded by an ideal octahedron of six Te atoms in PbTe. This is a consequence of the stereochemically active lone pair of $Tl^+$. It should also be noted that $Tl_9BiTe_6$ contains over 56 atomic-% Tl because of its +1 state, resulting in a higher averaged molar mass of 175.9 g $mol^{-1}$, compared to 167.4 g $mol^{-1}$ for PbTe and 160.2 g $mol^{-1}$ for $Bi_2Te_3$. Other substitution variants in polycrystalline form have matched or even exceeded this performance after optimizing the electron concentration, namely $Tl_9Bi_{0.98}Te_6$ [16], $Tl_{8.05}Sn_{1.95}Te_6$ and $Tl_{8.10}Pb_{1.90}Te_6$ [17] with $zT_{max}$ values ranging from 1.1 to 1.4.

As summarized in a review on group 13 chalcogenides [41], several other thallium tellurides exhibit very low thermal conductivity as well. Examples with figure of merit values in excess of unity include $TlAg_9Te_5$ with $zT_{max}$ = 1.2 at 700 K [42] and $Tl_2Ag_{12}Te_{7.4}$ with $zT_{max}$ = 1.1 at 520 K [18]. From the crystallographic point of view, $TlAg_9Te_5$ is better described as $Tl_{12}Ag_{96.5}Te_{66} \approx Tl_2Ag_{16}Te_{11}$, adopting a highly complex crystal structure with several deficient Ag positions with site occupancies between 46% and 88% [43]. The structure contains large hexagonal channels formed by the Ag and Te atoms, filled with chains of Tl atoms.

The same general description holds true for the structure of $Tl_2Ag_{12}Te_{7.4}$, a variant of the $Zr_2Fe_{12}P_7$ type [44], while the Ag site occupancies are generally higher. More precisely, $Tl_2Ag_{12}Te_{7.4}$ is described best as a composite structure, consisting of a composite I, the

$Tl_2Ag_{12}Te_6$ framework topologically equivalent with that part of $Zr_2Fe_{12}P_7$, and composite II, a distorted linear Te atom chain with about 1.4 Te atoms per $Tl_2Ag_{12}Te_6$ unit. Figure 1 depicts the sub cell of this material, where the Te chain is represented as the average of composite II, reflected in an equidistant chain of Te2 atoms with huge anisotropic displacement parameters.

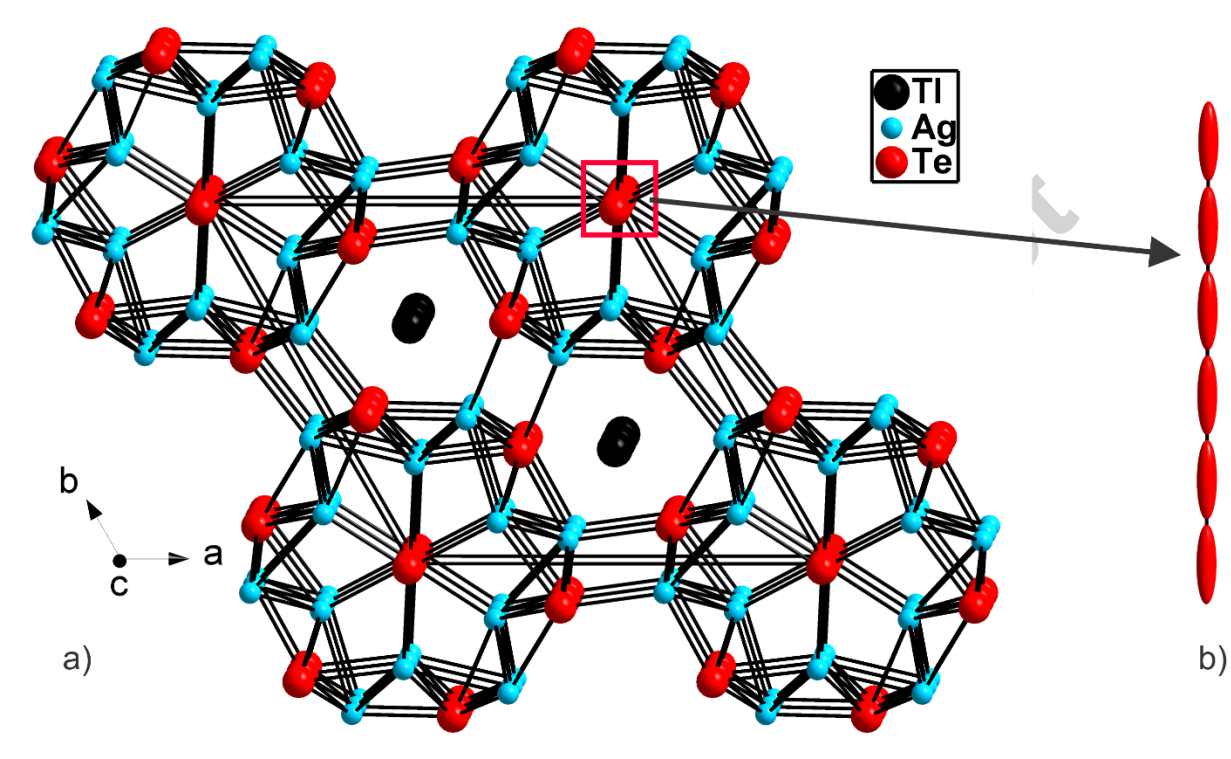


Figure 1. a) Sub cell of $Tl_2Ag_{12}Te_7$; b) ellipsoid representation of the linear Te2 chain on (0, 0, *z*). Reprinted with permission from ref. [18]. Copyright 2018 American Chemical Society.

Therein, the incommensurate distortion of the Te2 chain into $Te_2^{2-}$ and $Te_3^{4-}$ units has a strong impact onto the neighboring Ag atoms (Figure 2), and a smaller one on the next-nearest neighbors. Thus, large parts of the crystal structure are distorted, and the Ag deficiencies additionally further block the phonon propagation, resulting in an ultralow thermal conductivity of < 0.3 W $m^{-1}K^{-1}$.

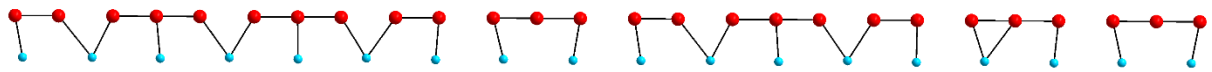

Figure 2. Section of the composite $Tl_2Ag_{12}Te_{7.4}$ structure along the modulation (*c*) axis comprising Te dimers and trimers (shown with the neighboring Ag atoms). Reprinted with permission from ref. [18]. Copyright 2018 American Chemical Society.

In both of these Tl-Ag tellurides, the low thermal conductivity is not so much a consequence of the distortion of the Tl-Te polyhedra, or of the high average molar masses, as the Tl concentration is small, but of the high complexity and the local distortions. Thus, these tellurides are perfect examples of the "phonon-glass electron-crystal" (PGEC) concept proposed by Slack [45].

Along with the Ag site deficiencies, multiple Ag–Ag contacts persist in these structures. Such $Cu^+$–$Cu^+$ and $Ag^+$–$Ag^+$ bonding contacts occur in several chalcogenides, including in $Ba_3Cu_{14-x}Te_{12}$ [46] and $BaAg_2Te_2$ ($\alpha$-$BaCu_2S_2$ type) with Ag–Ag distances of 2.9 Å in $AgTe_4$ chains [47]. Though formally closed-shell interactions ($d^{10}$–$d^{10}$), a bonding character arises from the hybridization of the *d* states with the nominally empty *s* and *p* orbitals of the Cu/Ag atoms [48–50]. Therefore, the Cu/Ag cations may exhibit ion mobility in these materials, further contributing to low thermal conductivity, as for example demonstrated for the "liquid-like" $Cu_2Se$ [51]. In fact, we found evidence for such Ag ion mobility in the case of the selenide $Tl_2Ag_{12}Se_7$ [52], which crystallizes in a supercell of the $Zr_2Fe_{12}P_7$ type.

## 4. Thermoelectric copper chalcogenides

### *4.1. Binary chalcogenides, $Cu_2Q$ with Q = S, Se, Te*

As summarized in a critical review in 2014, the interest in $Cu_2S$ as a thermoelectric dates back to the 19$^{th}$ century [53]. The usage of $Cu_2Se$, exhibiting a $zT_{max}$ = 1.5, in a thermoelectric device led to a system failure because of the Cu ion migration out of the thermoelectric leg in the late 1980s [54]. That occurrence has limited research into thermoelectric copper chalcogenides for several decades, until researchers began to search for concepts to impede the ion migration in attempts to maintain material stability [55]. Two recent reviews addressed this issue [56,57]. Before delving into that, we first present the structures and properties of the leading binary chalcogenides $Cu_2Q$ with $Q$ = S, Se, Te. These semiconductors with band gaps between 1.0 eV and 1.2 eV consist of a fixed framework of immobile $Q^{2-}$ anions, with the Cu ions occupying different holes thereof, leading to a variety of different structures and phase transitions.

The chalcocite $Cu_2S$ occurs in three different modifications, depending on the temperature. The low temperature form, the $\gamma$ phase, is monoclinic, which transforms into the hexagonal $\beta$ form at 370 K. The superionic cubic $\alpha$ phase [58], thermodynamically stable above 700 K, is comprised of a face-centered cubic sublattice of $S^{2-}$ ions, with the Cu ions located in many different positions with fractional occupancies (Figure 3). The latter is often described as a liquid-like sublattice. Various studies have consistently shown the lattice thermal conductivity being well below 0.8 W $m^{-1}K^{-1}$, despite the relatively low average molar mass of 53.1 g $mol^{-1}$.

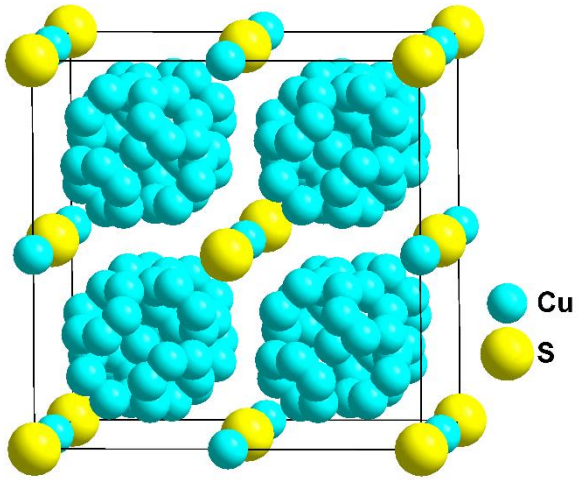


Figure 3. Crystal structure of $\alpha$-$Cu_2S$.

An investigation varying x in $Cu_{2-x}S$ found peak performance for $Cu_{1.97}S$ with $zT_{max}$ = 1.7 at 1000 K [59], a sensationally high value for a bulk sulfide. Using a melt-solidification technique, the performance was even further increased to $zT_{max}$ = 1.9 at 973 K [60]. Poor stability of that $Cu_{1.97}S$ was observed during the electrical measurements because of the high and unrestricted ion mobility, however.

$Cu_2S$ and $Cu_2Se$ form a solid solution over all S/Se ratios, which in part results in even lower thermal conductivity. Replacing small amounts of Se with S optimized (lowered) the charge carrier concentration of $Cu_2Se$ via reduction of the Cu vacancies by the stronger Cu–S bonds, causing a $zT$ = 2.0 at 1000 K in case of $Cu_2S_{0.08}Se_{0.92}$ after SPS [61]. $Cu_2S_{0.2}Se_{0.8}$ was reported to attain $zT$ = 1.65 at 950 K after SPS, exhibiting a lattice thermal conductivity < 0.4 W $m^{-1}K^{-1}$ throughout the whole temperature range [62]. An outstanding $zT_{max}$ was obtained with an S/Se ratio of 1 : 1, namely $zT$ = 2.3 at 1000 K in case of $Cu_{1.94}S_{0.5}Se_{0.5}$ after SPS [63]. These

samples are composed of different polymorphs on the mesoscale as well as various nanodomains.

Alloying with Te and using the concept of nanoscale mosaicity via spark-plasma-sintering, $zT$ was reported to reach 2.1 at 1000 K in the case of $Cu_2S_{0.52}Te_{0.48}$, with lattice thermal conductivity values being in the range of 0.3 W $m^{-1}K^{-1}$ to 0.4 W $m^{-1}K^{-1}$ [64]. The thermal conductivity and figure of merit plots are shown in Figure 4, along with those of $Cu_2Se$ and $Cu_2Te$.

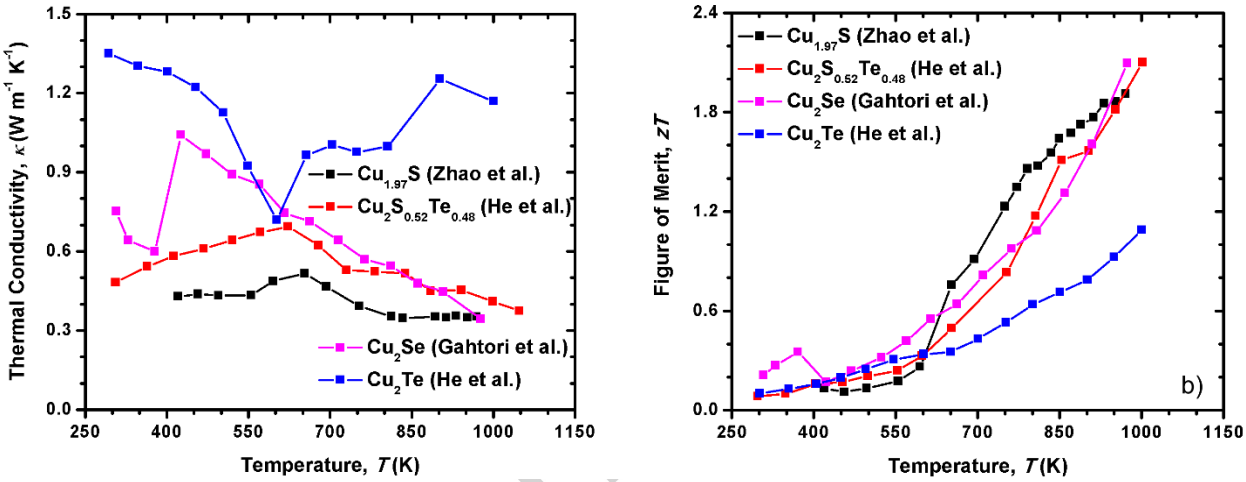


Figure 4. a) Thermal conductivity; b) figure of merit of selected $Cu_{2-x}Q$ materials.

$\alpha$-$Cu_2Se$ undergoes a phase transition around 410 K into the fast ion conducting $\beta$ form, wherein the Se atoms form a face-centered lattice with Cu atoms being kinetically disordered over various interstitial positions. Since 2012, various investigations have revealed high $zT_{max}$ values from 973 K to 1000 K, including $zT$ = 1.5 after traditional solid state synthesis [51], 1.6 after ball-milling [65], 1.8 after self-propagating synthesis [66], 1.8 after melt-quenching [67], and finally a $zT_{max}$ = 2.1 after inclusions of defects on the nanoscale [25].

With five different phases known, $Cu_2Te$ has the most phase transformations of the $Cu_2Q$ series. Interestingly, the telluride exhibits the lowest albeit still impressive thermoelectric performance of the $Cu_2Q$ materials. At the highest temperature, above 850 K, the cubic ε-phase persists, where the highest $zT$ values are found. Undoped $Cu_2Te$ was reported to only have a $zT_{max}$ = 0.29 at 900 K, while Ag-doping led to a substantial enhancement of $zT_{max}$ = 1.0 at 900 K

[68]. Subsequently it was shown that similar if not superior values – a $zT_{max}$ = 1.1 at 1000 K – can be achieved without Ag, namely via minimizing the carrier concentration [69].

While all of these superionic conductors have stability issues, introducing trace amounts of indium into $Cu_2Se$ led to the formation of nanocomposites $Cu_2Se/CuInSe_2$, which simultaneously enhanced the stability of the material under the measurement conditions as well as the thermoelectric performance. With 1 mole-% In, a huge $zT_{max}$ = 2.6 was obtained at 850 K [26].

A different concept to obtain the required stability was introduced in 2018, based on the idea that the ion conducting material must be kept under a critical chemical potential difference to prevents the ions (here: Cu ions) from precipitating out of the thermoelectric legs. For this, ion-blocking but electron-conducting interfaces were added to lower the critical voltages in the thereby created segments [70].

*4.2. Ternary and higher Cu chalcogenides*

We have been investigating Ba-containing copper chalcogenides since over a decade, anticipating that the large Ba cations would limit the Cu ion migration to a unit cell or a smaller Cu cluster therein [55]. To that extent, we demonstrated the stability of $BaCu_{6-x}QTe_6$ with $Q$ = S, Se [71]. Figure 5 illustrates that the Cu mobility is limited to a S/Se-centered cube of Cu atoms, where statistically 2+x Cu atoms are missing (with $0.1 \leq x \leq 0.3$) [72].

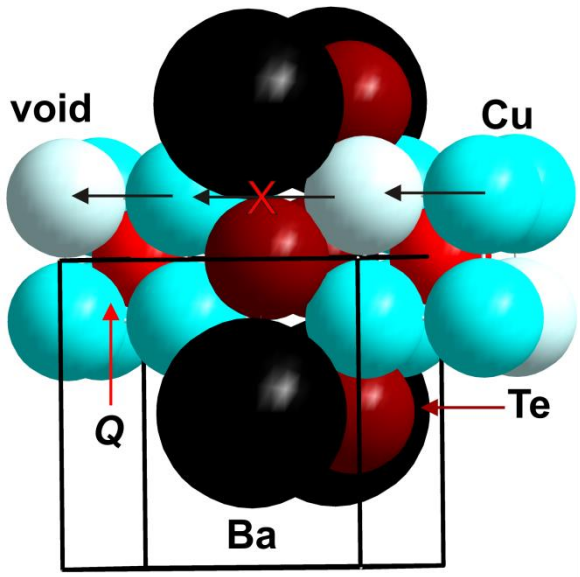

Figure 5. Part of the $BaCu_{6-x}QTe_6$ structure. Adapted with permission from ref. [72]. Copyright 2018 American Chemical Society.

This material too is bestowed with a low thermal conductivity < 0.8 W $m^{-1}K^{-1}$, caused by the Cu deficiencies and movements despite the simple small cubic cell and a low molar mass average compared to e.g. PbTe and $Bi_2Te_3$. The highest $zT$ found thus far in this family was 0.8 at 600 K [72].

Another interesting Cu-containing chalcogenide family is based on variants of the wurtzite or sphalerite structure, where different ordering of the cations leads to a number of different supercells of lower symmetry. Excellent examples for this are the chalcopyrites $CuGaTe_2$ and $CuInTe_2$, which adopt a tetragonal body-centered 1 × 1 × 2 supercell of the sphalerite. Compared to the materials discussed above, their room temperature thermal conductivity is relatively high with > 6 W $m^{-1}K^{-1}$, but it decreases down to below 1.0 W $m^{-1}K^{-1}$ above 800 K (Figure 6), postulated to be caused by the large anharmonicity. The figure of merit values at low temperatures are unimpressive, but raising the temperature leads to excellent performance with $zT_{max}$ = 1.4 at 950 K for $CuGaTe_2$ [73] and 1.2 at 850 K for $CuInTe_2$ [74] because of the high power factors and the large temperature dependence of the thermal conductivity. Similar performances were found for the related selenides $Cu_2ZnSn_{0.90}In_{0.10}Se$ with $zT_{max}$ = 0.95 at 850 K [75], $Cu_2Sn_{0.90}In_{0.10}Se_3$ with $zT_{max}$ = 1.1 at 850 K [76], and nanocrystalline $Cu_3Sn_{0.10}Sb_{0.88}Bi_{0.02}Se_4$ with $zT_{max}$ = 1.3 at 650 K [77].

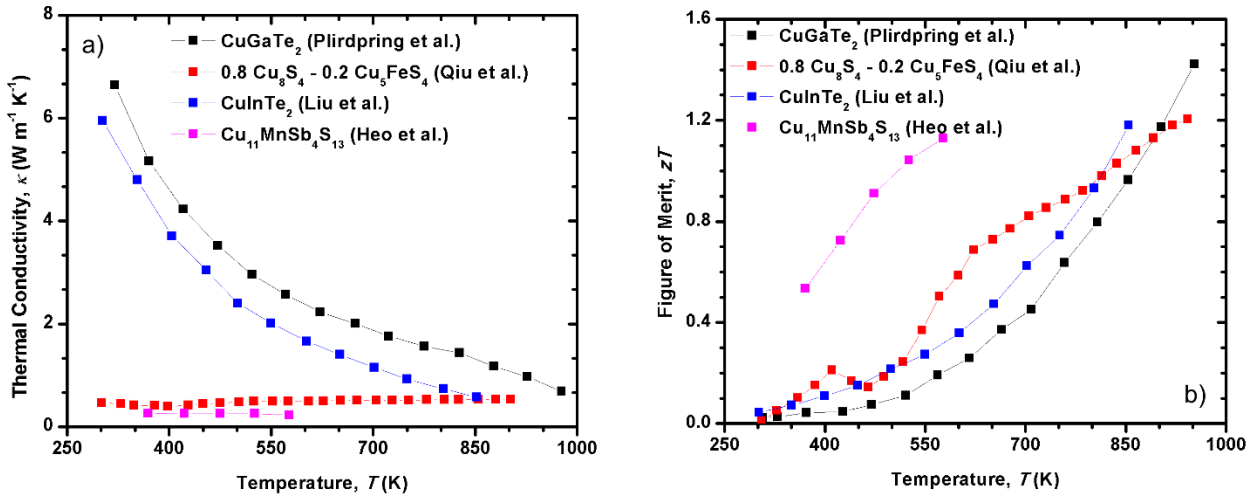

Figure 6. a) Thermal conductivity; b) figure of merit of selected ternary and higher copper chalcogenides.

In contrast to the above, $CuCrSe_2$ adopts a layered structure, which can be described based on anionic $CrSe_2^-$ layers of the $CdI_2$ type, with superionic $Cu^+$ atoms between the $CrSe_2^-$ layers. Amorphous nanodomains within the crystalline material contribute along with the superionic $Cu^+$ atoms to a very low thermal conductivity, which ultimately results in a competitive figure of merit of 1.0 at 773 K [78].

Last but not least, minerals based on copper sulfides were recently shown to exhibit good thermoelectric properties as well. The tetrahedrites $Cu_{12-x}M_xSb_4S_{13}$ (*M* = Mn, Fe, Co, Ni, Zn, Hg) crystallize in the complex cubic unit cell shown in Figure 7. In this structure, the Sb coordination is heavily distorted because of the lone pair effect of $Sb^{3+}$, and one Cu atom is only bonded to three S atoms. This causes a large anharmonicity, and – along with the large unit cell – a low lattice thermal conductivity, often below 0.6 W $m^{-1}K^{-1}$ despite this being a sulfide and not a telluride [79]. Additional complexity arises from the fact that tetrahedrites can be Cu-rich, as expressed in the formula $Cu_{12+x}Sb_4S_{13}$ with $x < 2$. The Cu-rich tetrahedrite becomes ion conducting above 393 K, occurring with lower thermal conductivity and higher figure of merit, e.g. ≈ 0.62 at 573 K for x = 2, compared with ≈ 0.4 for x = 0 [80].

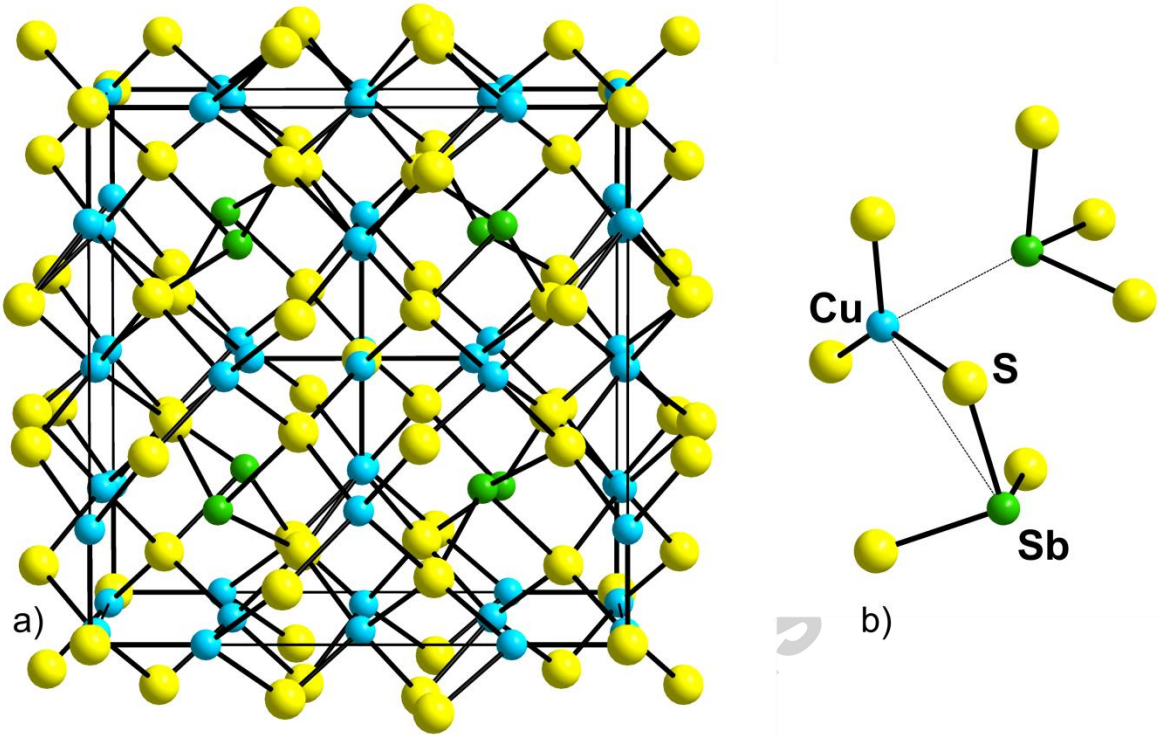


Figure 7. a) Crystal structure of $Cu_{12}Sb_4S_{13}$; b) its peculiar $CuSb_2S_8$ unit.

$Cu_{12-x}Zn_xSb_4S_{13}$ is an intrinsic semiconductor when x = 2; the material turns into a *p*-doped semiconductor with smaller x values. Optimizing the carrier (hole) concentration via adjusting x led to a $zT_{max}$ = 0.95 at 700 K [81]. Interestingly, as reported in the same article, competitive properties with $zT_{max} \approx 0.6$ were achieved after hot-pressing of a mixture of freshly synthesized $Cu_{12}Sb_4S_{13}$ and the commercial tennantite $Cu_{10.5}Fe_{1.5}As_{3.6}Sb_{0.4}S_{13}$. To date, the best performing tetrahedrite is $Cu_{11}MnSb_4S_{13}$ with $zT_{max}$ = 1.1 at 575 K [82], as depicted in Figure 6.

Other Cu-S minerals under investigation are the colusites and the bornite. Colusites are $Cu_{26}V_2M_6S_{32}$ (with *M* = Ge, Sn, As, Sb), that also adopt a large cubic unit cell with low thermal conductivity. Currently the best performing materials in this family are $Cu_{26}Ta_2Sn_{5.5}S_{32}$ and $Cu_{26}Nb_2Ge_6S_{32}$, both with $zT_{max}$ = 1.0 at 670 K [83].

Bornite is $Cu_5FeS_4$, whose cubic high temperature modification can be described based on $Cu_2S$, with one of eight Cu atoms replaced by Fe and two by vacancies □, according to $Cu_5Fe□_2S_4$. Its lattice thermal conductivity is around 0.5 W $m^{-1}K^{-1}$ above room temperature [84], caused by the Cu ion conduction and the deficiencies. The immobile Fe atoms appear to

limit the Cu ion migration and thus increase the material's stability. Via adjusting the carrier concentration by decreasing the Cu and Fe content, a $zT_{max}$ = 0.79 at 550 K was achieved for $Cu_{4.972}Fe_{0.968}S_4$ [85]. Solid solutions of $Cu_2S$ ($Cu_8S_4$) and $Cu_5FeS_4$ were also investigated, which resulted in maximized performance in case of 0.8 $Cu_8S_4$ – 0.2 $Cu_5Fe\square_2S_4$, mostly a consequence of an increased electrical conductivity and a basically unchanged Seebeck coefficient [84]. Its maximum *zT* of 1.2 was found at the end of the investigated temperature range, namely at 900 K (Figure 6).

## 4. Conclusions

As demonstrated in this review, it is possible to move away from toxic and expensive heavy metal tellurides to affordable and more benign sulfides and selenides while retaining the desired low thermal conductivity and high thermoelectric performance. The variety of other methods to achieve low thermal conductivity in bulk materials includes incommensurate composite structures, local distortions via stereochemically active lone electron pairs, site deficiencies, superstructures caused by different cation ordering, and last but not least cation diffusion as in various copper chalcogenides leading to many additional, fractionally occupied Cu atom sites.

The Cu ion diffusion may lead to device instability, and must therefore be controlled. Possible mechanisms include immobile cations blocking the Cu path, as demonstrated for Ba, Fe, and In, as well as segmentation of the thermoelectric legs with ion blocking interfaces between the segments.

These recent developments may very well pave the path towards increased usages of thermoelectric materials. In fact, Alpha Energy has already begun utilizing tetrahedrites for TE energy generation from waste heat.



## Acknowledgments

Financial support from the Natural Sciences and Engineering Research Council of Canada is appreciated.

## References

[1] J. He, T.M. Tritt, Advances in thermoelectric materials research: Looking back and moving forward., Science. 357 (2017) eaak9997/1-9.

[2] D.M. Rowe, CRC Handbook of Thermoelectrics, CRC Press, Boca Raton, FL, 1995.
[3] D.M. Rowe, Thermoelectrics Handbook: Macro to Nano, CRC Press, Taylor & Francis Group, Boca Raton, FL, USA, 2006.
[4] R.R. Furlong, E.J. Wahlquist, US space missions using radioisotope power systems, Nucl. News. 42 (1999) 26–35.
[5] J. Yang, T. Caillat, Thermoelectric Materials for Space and Automotive Power Generation, MRS Bull. 31 (2006) 224–229.
[6] J. Yang, F.R. Stabler, Automotive Applications of Thermoelectric Materials, J. Electron. Mater. 38 (2009) 1245–1251.
[7] M. Matsumoto, M. Mori, T. Haraguchi, M. Ohtani, T. Kubo, K. Matsumoto, H. Matsuda, Development of State of the Art Compact and Lightweight Thermoelectric Generator Using Vacuum Space Structure, SAE Int. J. Engines. 8 (2015) 1815–1825.
[8] B. Orr, A. Akbarzadeh, M. Mochizuki, R. Singh, A review of car waste heat recovery systems utilising thermoelectric generators and heat pipes, Appl. Therm. Eng. 101 (2016) 490–495.
[9] G.J. Snyder, E.S. Toberer, Complex thermoelectric materials, Nat. Mater. 7 (2008) 105–114.
[10] H. Kleinke, New bulk Materials for Thermoelectric Power Generation: Clathrates and Complex Antimonides, Chem. Mater. 22 (2010) 604–611.
[11] X. Shi, J. Yang, J.R. Salvador, M. Chi, J.Y. Cho, H. Wang, S. Bai, J. Yang, W. Zhang, L. Chen, Multiple-Filled Skutterudites: High Thermoelectric Figure of Merit through Separately Optimizing Electrical and Thermal Transports, J. Am. Chem. Soc. 133 (2011) 7837–7846.
[12] X. Shi, J. Yang, S. Bai, J. Yang, H. Wang, M. Chi, J.R. Salvador, W. Zhang, L. Chen, W. Wong-Ng, On the Design of High-Efficiency Thermoelectric Clathrates through a Systematic Cross-Substitution of Framework Elements, Adv. Funct. Mater. 20 (2010) 755–763.
[13] E.S. Toberer, C.A. Cox, S.R. Brown, T. Ikeda, A.F. May, S.M. Kauzlarich, G.J. Snyder, Traversing the Metal-Insulator Transition in a Zintl Phase: Rational Enhancement of Thermoelectric Efficiency in Yb14Mn1-xAlxSb11, Adv. Funct. Mater. 18 (2008) 2795–2800.
[14] N. Shutoh, S. Sakurada, Thermoelectric properties of the Tix(Zr0.5Hf0.5)1-xNiSn half-Heusler compounds, J. Alloy. Compd. 389 (2005) 204–208.
[15] T. Caillat, J.-P. Fleurial, A. Borshchevsky, Preparation and thermoelectric properties of semiconducting Zn4Sb3, J. Phys. Chem. Solids. 58 (1997) 1119–1125.
[16] Q. Guo, M. Chan, B.A. Kuropatwa, H. Kleinke, Enhanced thermoelectric properties of variants of Tl9SbTe6 and Tl9BiTe6, Chem. Mater. 25 (2013) 4097–4104.
[17] Q. Guo, A. Assoud, H. Kleinke, Improved Bulk Materials with Thermoelectric Figure-of-Merit > 1: Tl10–xSnxTe6 and Tl10–xPbxTe6, Adv. Energy Mater. 4 (2014) 1400348/1-8.
[18] Y. Shi, A. Assoud, S. Ponou, S. Lidin, H. Kleinke, A New Material with a Composite Crystal Structure Causing Ultralow Thermal Conductivity and Outstanding Thermoelectric Properties: Tl2Ag12Te7+δ, J. Am. Chem. Soc. 140 (2018) 8578–8585.
[19] J.P. Heremans, V. Jovovic, E.S. Toberer, A. Saramat, K. Kurosaki, A. Charoenphakdee, S. Yamanaka, G.J. Snyder, Enhancement of Thermoelectric Efficiency in PbTe by Distortion of the Electronic Density of States, Science. 321 (2008) 554–557.
[20] F. Wu, H. Song, F. Gao, W. Shi, J. Jia, X. Hu, Effects of different morphologies of

Bi2Te3 nanopowders on thermoelectric properties, J. Electron. Mater. 42 (2013) 1140–1145.
[21] R. Venkatasubramanian, E. Slivola, T. Colpitts, B. O'Quinn, Thin-film thermoelectric devices with high room-temperature figures of merit, Nature. 413 (2001) 597–602.
[22] K. Hsu, S. Loo, F. Guo, W. Chen, J. Dyck, C. Uher, T. Hogan, E. Polychroniadis, M. Kanatzidis, Cubic AgPbmSbTe2+m: Bulk Thermoelectric Materials with High Figure of Merit, Science. 303 (2004) 818–821.
[23] K. Biswas, J. He, I.D. Blum, C.-I. Wu, T.P. Hogan, D.N. Seidman, V.P. Dravid, M.G. Kanatzidis, High-performance bulk thermoelectrics with all-scale hierarchical architecture, Nature. 489 (2012) 414–418.
[24] T.C. Harman, M.P. Walsh, B.E. Laforge, G.W. Turner, Nanostructured thermoelectric materials, J. Electron. Mater. 34 (2005) L19–L22.
[25] B. Gahtori, S. Bathula, K. Tyagi, M. Jayasimhadri, A.K. Srivastava, S. Singh, R.C. Budhani, A. Dhar, Giant enhancement in thermoelectric performance of copper selenide by incorporation of different nanoscale dimensional defect features, Nano Energy. 13 (2015) 36–46.
[26] A.A. Olvera, N.A. Moroz, P. Sahoo, P. Ren, T.P. Bailey, A.A. Page, C. Uher, P.F.P. Poudeu, Partial indium solubility induces chemical stability and colossal thermoelectric figure of merit in Cu2Se, Energy Environ. Sci. 10 (2017) 1668–1676.
[27] A.D. LaLonde, Y. Pei, H. Wang, G. Jeffrey Snyder, Lead telluride alloy thermoelectrics, Mater. Today. 14 (2011) 526–532.
[28] Y. Gelbstein, Z. Dashevsky, M.P. Dariel, High performance n-type PbTe-based materials for thermoelectric applications, Phys. B. 363 (2005) 196–205.
[29] Y. Pei, A. LaLonde, S. Iwanaga, G.J. Snyder, High thermoelectric figure of merit in heavy hole dominated PbTe, Energy Environ. Sci. 4 (2011) 2085–2089.
[30] E. Quarez, K.-F. Hsu, R. Pcionek, N. Frangis, E.K. Polychroniadis, M.G. Kanatzidis, Nanostructuring, Compositional Fluctuations, and Atomic Ordering in the Thermoelectric Materials AgPbmSbTe2+m. The Myth of Solid Solutions, J. Am. Chem. Soc. 127 (2005) 9177–9190.
[31] J. Androulakis, C.-H. Lin, H.-J. Kong, C. Uher, C.-I. Wu, T. Hogan, B.A. Cook, T. Caillat, K.M. Paraskevopoulos, M.G. Kanatzidis, Spinodal Decomposition and Nucleation and Growth as a Means to Bulk Nanostructured Thermoelectrics: Enhanced Performance in Pb1-xSnxTe−PbS, J. Am. Chem. Soc. 129 (2007) 9780–9788.
[32] L.-D. Zhao, C. Chang, G. Tan, M.G. Kanatzidis, SnSe: a remarkable new thermoelectric material, Energy Environ. Sci. Energy Environ. Sci. 9 (2016) 3044–3060.
[33] L.-D. Zhao, S.-H. Lo, Y. Zhang, H. Sun, G. Tan, C. Uher, C. Wolverton, V.P. Dravid, M.G. Kanatzidis, Ultralow thermal conductivity and high thermoelectric figure of merit in SnSe crystals, Nature. 508 (2014) 373–377.
[34] Y. Fu, J. Xu, G.-Q. Liu, J. Yang, X. Tan, Z. Liu, H. Qin, H. Shao, H. Jiang, B. Liang, J. Jiang, Enhanced thermoelectric performance in p-type polycrystalline SnSe benefiting from texture modulation, J. Mater. Chem. C. 4 (2016) 1201–1207.
[35] X. Shi, Z.-G. Chen, W. Liu, L. Yang, M. Hong, R. Moshwan, L. Huang, J. Zou, Achieving high Figure of Merit in p-type polycrystalline Sn0.98Se via self-doping and anisotropy-strengthening, Energy Storage Mater. 10 (2018) 130–138.
[36] T.C. Harman, B. Paris, S.E. Miller, H.L. Goering, Preparation and some physical properties of Bi2Te3, Sb2Te3, and As2Te3, J. Phys. Chem. Solids. 2 (1957) 181–190.

[37] F. Hao, P. Qiu, Y. Tang, S. Bai, T. Xing, H.-S. Chu, Q. Zhang, P. Lu, T. Zhang, D. Ren, J. Chen, X. Shi, L. Chen, High efficiency Bi2Te3-based materials and devices for thermoelectric power generation between 100 and 300 °C, Energy Environ. Sci. 9 (2016) 3120–3127.
[38] J.-J. Shen, T.-J. Zhu, X.-B. Zhao, S.-N. Zhang, S.-H. Yang, Z.-Z. Yin, Recrystallization induced in situ nanostructures in bulk bismuth antimony tellurides: a simple top down route and improved thermoelectric properties, Energy Environ. Sci. 3 (2010) 1519–1523.
[39] H.Y. Lv, H.J. Liu, J. Shi, X.F. Tang, C. Uher, Optimized thermoelectric performance of Bi2Te3 nanowires, J. Mater. Chem. A. 1 (2013) 6831–6838.
[40] B. Wölfing, C. Kloc, J. Teubner, E. Bucher, High performance thermoelectric Tl9BiTe6 with an extremely low thermal conductivity, Phys. Rev. Lett. 86 (2001) 4350–4353.
[41] K. Kurosaki, S. Yamanaka, Low-thermal-conductivity group 13 chalcogenides as high-efficiency thermoelectric materials, Phys. Status Solidi. 210 (2013) 82–88.
[42] K. Kurosaki, A. Kosuga, H. Muta, M. Uno, S. Yamanaka, Ag9TlTe5: A high-performance thermoelectric bulk material with extremely low thermal conductivity, Appl. Phys. Lett. 87 (2005) 3–5.
[43] D. Paccard, L. Paccard, G. Brun, J.C. Tedenac, A new phase in the Tl-Ag-Te system: crystal structure of Tl2Ag16Te11, J. Alloy. Compd. 184 (1992) 337–342.
[44] E. Ganglberger, Die Kristallstruktur von Fe12Zr2P7, Monatsh. Chem. 99 (1968) 557–568.
[45] G.A. Slack, New Materials and Performance Limits for Thermoelectric Cooling, in: D.M. Rowe (Ed.), CRC Handb. Thermoelectr., CRC Press, Boca Raton, FL, 1995: pp. 407–440.
[46] A. Assoud, S. Thomas, B. Sutherland, H. Zhang, T.M. Tritt, H. Kleinke, Thermoelectric Properties of the New Polytelluride Ba3Cu14-dTe12, Chem. Mater. 18 (2006) 3866–3872.
[47] A. Assoud, Y. Cui, S. Thomas, B. Sutherland, H. Kleinke, Structure and Physical Properties of the new telluride BaAg2Te2 and its quaternary variants BaCudAg2–dTe2, J. Solid State Chem. 181 (2008) 2024–2030.
[48] P.K. Mehrotra, R. Hoffmann, Copper(I)-copper(I) interactions. Bonding relationships in d10-d10 systems, Inorg. Chem. 17 (1978) 2187–2189.
[49] K.M. Merz Jr., R. Hoffmann, d10-d10 Interactions: multinuclear copper(I) complexes, Inorg. Chem. 27 (1988) 2120–2127.
[50] P. Pyykkö, Strong closed shell interactions, Chem. Rev. 97 (1997) 597–636.
[51] H. Liu, X. Shi, F. Xu, L. Zhang, W. Zhang, L. Chen, Q. Li, C. Uher, T. Day, G. Snyder Jeffrey, Copper ion liquid-like thermoelectrics, Nat. Mater. 11 (2012) 422–425.
[52] Y. Shi, A. Assoud, C.R. Sankar, H. Kleinke, TlAg12Se7: A New pnp Conduction Switching Material with Extraordinarily Low Thermal Conductivity, Chem. Mater. 29 (2017) 9565–9571.
[53] G. Dennler, R. Chmielowski, S. Jacob, F. Capet, P. Roussel, S. Zastrow, K. Nielsch, I. Opahle, G.K.H. Madsen, Are Binary Copper Sulfides/Selenides Really New and Promising Thermoelectric Materials?, Adv. Energy Mater. 4 (2014) 1301581/1-12.
[54] D.R. Brown, T. Day, T. Caillat, G.J. Snyder, Chemical stability of (Ag,Cu)2Se: a historical overview, J. Electron. Mater. 42 (2013) 2014–2019.
[55] O. Mayasree, C.R. Sankar, K.M. Kleinke, H. Kleinke, Cu Clusters and Chalcogen–Chalcogen Bonds in Various Copper Polychalcogenides, Coord. Chem. Rev. 256 (2012) 1377–1383.
[56] P. Qiu, X. Shi, L. Chen, Cu-based thermoelectric materials, Energy Storage Mater. 3 (2016) 85–97.

[57] T.-R. Wei, Y. Qin, T. Deng, Q. Song, B. Jiang, R. Liu, P. Qiu, X. Shi, L. Chen, Copper chalcogenide thermoelectric materials, Sci. China Mater. 5 (2018) 1–17.
[58] M.K. Balapanov, I.G. Gafurov, U.K. Mukhamed'yanov, R.A. Yakshibaev, R.K. Ishembetov, Ionic conductivity and chemical diffusion in superionic LixCu2−xS (0≤x≤ 0.25), Phys. Status Solidi B. 241 (2004) 114–119.
[59] Y. He, T. Day, T. Zhang, H. Liu, X. Shi, L. Chen, G.J. Snyder, High Thermoelectric Performance in Non-Toxic Earth-Abundant Copper Sulfide, Adv. Mater. 26 (2014) 3974–3978.
[60] L. Zhao, X. Wang, F.Y. Fei, J. Wang, Z. Cheng, S. Dou, J. Wang, G.J. Snyder, High thermoelectric and mechanical performance in highly dense Cu2-xS bulks prepared by a melt-solidification technique, J. Mater. Chem. A. 3 (2015) 9432–9437.
[61] K. Zhao, A.B. Blichfeld, H. Chen, Q. Song, T. Zhang, C. Zhu, D. Ren, R. Hanus, P. Qiu, B.B. Iversen, F. Xu, G.J. Snyder, X. Shi, L. Chen, Enhanced Thermoelectric Performance through Tuning Bonding Energy in Cu2Se1− xSx Liquid-like Materials, Chem. Mater. 29 (2017) 6367–6377.
[62] K. Zhao, A.B. Blichfeld, E. Eikeland, P. Qiu, D. Ren, B.B. Iversen, X. Shi, L. Chen, Extremely low thermal conductivity and high thermoelectric performance in liquid-like Cu2Se1−xSx polymorphic materials, J. Mater. Chem. A. 5 (2017) 18148–18156.
[63] K. Zhao, P. Qiu, Q. Song, A.B. Blichfeld, E. Eikeland, D. Ren, B. Ge, B.B. Iversen, X. Shi, L. Chen, Ultrahigh thermoelectric performance in Cu2−ySe0.5S0.5 liquid-like materials, Mater. Today Phys. 1 (2017) 14–23.
[64] Y. He, P. Lu, X. Shi, F. Xu, T. Zhang, G.J. Snyder, C. Uher, L. Chen, Ultrahigh Thermoelectric Performance in Mosaic Crystals, Adv. Mater. 27 (2015) 3639–3644.
[65] B. Yu, W. Liu, S. Chen, H. Wang, H. Wang, G. Chen, Z. Ren, Thermoelectric properties of copper selenide with ordered selenium layer and disordered copper layer, Nano Energy. 1 (2012) 472–478.
[66] X. Su, F. Fu, Y. Yan, G. Zheng, T. Liang, Q. Zhang, X. Cheng, D. Yang, H. Chi, X. Tang, Q. Zhang, C. Uher, Self-propagating high-temperature synthesis for compound thermoelectrics and new criterion for combustion processing., Nat. Commun. 5 (2014) 4908/1-7.
[67] L. Zhao, X. Wang, J. Wang, Z. Cheng, S. Dou, J. Wang, L. Liu, Superior intrinsic thermoelectric performance with zT of 1.8 in single-crystal and melt-quenched highly dense Cu2-xSe bulks, Sci. Rep. 5 (2015) 7671/1-6.
[68] S. Ballikaya, H. Chi, J.R. Salvador, C. Uher, Thermoelectric properties of Ag-doped Cu2Se and Cu2Te, J. Mater. Chem. A. 1 (2013) 12478–12484.
[69] Y. He, T. Zhang, X. Shi, S.-H. Wei, L. Chen, High thermoelectric performance in copper telluride, NPG Asia Mater. 7 (2015) e210/1-7.
[70] P. Qiu, M.T. Agne, Y. Liu, Y. Zhu, H. Chen, T. Mao, J. Yang, W. Zhang, S.M. Haile, W.G. Zeier, J. Janek, C. Uher, X. Shi, L. Chen, G.J. Snyder, Suppression of atom motion and metal deposition in mixed ionic electronic conductors, Nat. Commun. 9 (2018) 4–11.
[71] O. Mayasree, C.R. Sankar, Y. Cui, A. Assoud, H. Kleinke, Synthesis, Structure and Thermoelectric Properties of Barium Copper Polychalcogenides with Chalcogen-Centered Cu Clusters and Te22– Dumbbells, Eur. J. Inorg. Chem. (2011) 4037–4042.
[72] M. Oudah, K.M. Kleinke, H. Kleinke, Thermoelectric Properties of the Quaternary Chalcogenides BaCu5.9STe6 and BaCu5.9SeTe6, Inorg. Chem. 54 (2015) 845–849.
[73] T. Plirdpring, K. Kurosaki, A. Kosuga, T. Day, S. Firdosy, V. Ravi, G.J. Snyder, A.

Harnwunggmoung, T. Sugahara, Y. Ohishi, H. Muta, S. Yamanaka, Chalcopyrite CuGaTe2: A High-Efficiency Bulk Thermoelectric Material, Adv. Mater. 24 (2012) 3622–3626.

[74] R. Liu, L. Xi, H. Liu, X. Shi, W. Zhang, L. Chen, Ternary compound CuInTe2: a promising thermoelectric material with diamond-like structure, Chem. Commun. 48 (2012) 3818–3820.

[75] X.Y. Shi, F.Q. Huang, M.L. Liu, L.D. Chen, Thermoelectric properties of tetrahedrally bonded wide-gap stannite compounds Cu2 ZnSn1-x Inx Se4, Appl. Phys. Lett. 94 (2009) 4–6.

[76] X. Shi, L. Xi, J. Fan, W. Zhang, L. Chen, Cu−Se Bond Network and Thermoelectric Compounds with Complex Diamondlike Structure, Chem. Mater. 22 (2010) 6029–6031.

[77] Y. Liu, G.G. García, S. Ortega, D. Cadavid, P. Palacios, J. Lu, M. Ibáñez, L. Xi, J. De Roo, A.M. López, S. Martí-Sánchez, I. Cabezas, M. de la Mata, Z. Luo, C. Dun, O. Dobrozhan, D.L. Carroll, W. Zhang, J. Martins, M. V Kovalenko, J. Arbiol, G. Noriega, J. Song, P. Wahnón, A. Cabot, Solution-based synthesis and processing of Sn-and Bi-doped Cu3SbSe4 nanocrystals, nanomaterials and ring-shaped thermoelectric generators, J. Mater. Chem. A. 5 (2017) 2592–2602.

[78] S. Bhattacharya, R. Basu, R. Bhatt, S. Pitale, A. Singh, D.K. Aswal, S.K. Gupta, M. Navaneethan, Y. Hayakawa, CuCrSe2: A high performance phonon glass and electron crystal thermoelectric material, J. Mater. Chem. A. 1 (2013) 11289–11294.

[79] R. Chetty, A. Bali, R.C. Mallik, Tetrahedrites as thermoelectric materials: an overview, J. Mater. Chem. C. 3 (2015) 12364–12378.

[80] P. Vaqueiro, G. Guélou, A. Kaltzoglou, R.I. Smith, T. Barbier, E. Guilmeau, A. V. Powell, The Influence of Mobile Copper Ions on the Glass-Like Thermal Conductivity of Copper-Rich Tetrahedrites, Chem. Mater. 29 (2017) 4080–4090.

[81] X. Lu, D.T. Morelli, Y. Xia, F. Zhou, V. Ozolins, H. Chi, X. Zhou, C. Uher, High Performance Thermoelectricity in Earth- Abundant Compounds Based on Natural Mineral Tetrahedrites, Adv. Energy Mater. 3 (2013) 342–348.

[82] J. Heo, G. Laurita, S. Muir, M.A. Subramanian, D.A. Keszler, Enhanced Thermoelectric Performance of Synthetic Tetrahedrites, Chem. Mater. 26 (2014) 2047–2051.

[83] Y. Bouyrie, M. Ohta, K. Suekuni, Y. Kikuchi, P. Jood, A. Yamamoto, T. Takabatake, Enhancement in the thermoelectric performance of colusites Cu26A2E6S32 (A = Nb, Ta; E = Sn, Ge) using E-site non-stoichiometry, J. Mater. Chem. C. 5 (2017) 4174–4184.

[84] P. Qiu, T. Zhang, Y. Qiu, X. Shi, L. Chen, Sulfide bornite thermoelectric material: A natural mineral with ultralow thermal conductivity, Energy Environ. Sci. 7 (2014) 4000–4006.

[85] S.O.J. Long, A. V. Powell, P. Vaqueiro, S. Hull, High Thermoelectric Performance of Bornite through Control of the Cu(II) Content and Vacancy Concentration, Chem. Mater. 30 (2018) 456–464.

**Highlights.**

- Recent progress in thermoelectric materials is presented.
- Outstanding thermoelectric performance depends strongly on the thermal conductivity.
- Heavy elements are not required to achieve the required low thermal conductivity.
- Stereochemically active lone pairs may result in low thermal conductivity.
- Ion mobility also leads to low thermal conductivity, but may be detrimental to device stability.